~~45896~~4

24p.

SAO and Kelvin waves in the EuroGRIPS GCMS and the UK Meteorological Office analyses

M. Amodei[1], S. Pawson[2,3], A.A. Scaife[4], W. Lahoz[5], U. Langematz[6], Ding Min Li[4], P. Simon[1]

January 27, 2000

Abstract

This work is an intercomparison of four tropospheric-stratospheric climate models, the Unified Model (UM) of the U.K. Meteorological Office (UKMO), the model of the Free University in Berlin (FUB), the ARPEGE-climat model of the National Center for Meteorological Research (CNRM), and the Extended UGAMP GCM (EUGCM) of the Center for Global Atmospheric Modelling (CGAM), against the UKMO analyses. This comparison has been made in the framework of the 'GSM-Reality Intercomparison Project for SPARC' (GRIPS). SPARC (Stratospheric Processes and their Role in Climate) aims are to investigate the effects of the middle atmosphere on climate and the GRIPS purpose is to organized a comprehensive assessment of current Middle Atmosphere-Climate Models (MACMs). The models integrations were made without identical contraints (e.g., boundary conditions, incoming solar radiation). All models are able to represent the dominant features of the extratropical circulation. In this paper, the structure of the tropical winds and the strengths of the Kelvin waves are examined. Explanations for the differences exhibited. between the models, as well as between models and analyses, are also proposed. In the analyses a rich spectrum of waves (eastward and westward) is present and contributes to drive the SAO (SemiAnnual Oscillation) and the QBO (Quasi-Biennal Oscillation). The amplitude of the Kelvin waves is close to the one observed in UARS (Upper Atmosphere Research Satellite) data. In agreement with observations, the Kelvin waves generated in the models propagate into the middle atmosphere as wave packets which underlines convective forcing origin. In most models, slow Kelvin waves propagate too high and are hence overestimated in the upper stratosphere and in the mesosphere, except for the UM which is more diffusive. These waves are not sufficient to force realistic westerlies of the QBO or SAO westerly phases. If the SAO is represented by all models only two of them are able to generate westerlies between 10 hPa and 50 hPa. The importance of the role played by subgrided gravity waves is more and more recognized. Actually, the EUGCM which includes a parametrization of gravity waves with a non-zero phase speed is able to simulate, with however some unrealistic features, clear easterly to westerly transitions as well as westerlies downward propagations. Thermal damping is also important in the westerlies forcing in the stratosphere. The model ARPEGE-climat shows more westerlies in the stratosphere than the other three models probably due to the use of a simplified scheme to predict the ozone distribution in the middle atmosphere.

Corresponding author address:
M. Amodei
CNRM/GMGEC/ERAM
42 Av. G. Coriolis, 31057 TOULOUSE Cedex, FRANCE
Tel: +33 5 6 07 93 50
Email: marielle.amodei@meteo.fr

Affiliations:
[1] CNRM. Météo France. Toulouse France
[2] Data Assimilation Office. NASA GSFC. Greenbelt,MD USA
[3] Universities Space Research Association. Seabrook, MD, USA
[4] United Kingdom Meteorological Office. Bracknell, UK
[5] Center for Global Atmospheric Modelling, University of Reading. UK
[6] Freie Universität Berlin. Germany

1 Introduction

The importance of the role played by the middle atmosphere in forcing the climate system is becoming more recognised. The World Climate Research Programme (WCRP) have reacted to this by initiating the 'Stratospheric Processes and their Role in Climate (SPARC)' research project (WCRP 1993. 1998), which is investigating the mechanisms through which the middle atmosphere exerts an influence on climate.

Middle Atmosphere-Climate Models (MACMs), which include representations of all physical processes thought to be relevant to the atmospheric circulation can be used to clarify the role the middle atmosphere plays in climate; in particular they can be used to determine how the tropospheric climate responds to middle atmospheric changes and how the system might evolve in the future. The 'GCM-Reality Intercomparison Project for SPARC' (GRIPS). including an European subgroup EuroGRIPS, is organizing a comprehensive assessment of current MACMs. While most models can simulate the dominant features of the extratropical circulation, there are considerable differences between the MACMs and some significant departures from reality (Pawson 1999). These deficiencies in the simulations extend to the tropical middle atmosphere. where many models have difficulty in representing the westerly phase of the SemiAnnual Oscillation (SAO) near the stratopause, and almost no models show a Quasi-Biennial Oscillation-like (QBO) signal.

It is now generally accepted that the QBO is forced by upward propagating waves, along the lines proposed by Lindzen and Holton (1968) and Holton and Lindzen (1972). Requirements for models to be able to capture such wave-forced motions include an adequate vertical resolution to represent the shear zones and the vertical wavelengths, as well as a generation mechanism for a tropical wave spectrum (Takahashi 1996; Horinouchi and Yoden 1997). Additionally, Takahashi (1996) found that it was necessary to reduce the strength of the horizontal diffusion.

The SAO discovery by Reed (1966) has been followed by many other works. As for the QBO, the generation of westerly winds requires a wave-mean flow interaction. It has been now confirmed from rocket and satellite observations that high-phase-speed Kelvin waves do propagate into the mesosphere and. along gravity-wave, are involved in the downward-propagating westerly acceleration (Hitchman and Leovy 1988). The mecanism driving the SAO easterly phase is completly different. The occurrence of simultaneous accelerations in a deep layer center near the stratopause suggests that the source is meridionnally propagating rather than vertically propagating. Mahlman and Umscheid (1984) verified with a high-resolution general circulation model that the easterly acceleration was due to a combination of planetary-wave forcing and mean advection.

Kelvin waves in the lower stratosphere were first detected in 1968 by Wallace and Kousky, in radiosonde records from three equatorial stations. From the linear theory of equatorial waves (e.g. Holton, 1975) the meridional wind associated with the Kelvin waves is null while the zonal wind, the geopotential and the temperature perturbations are symmetric about the equator. The Kelvin waves propagate Eastwards. Their phase velocity is directed downwards, while the group velocity is directed upwards. In the presence of a vertical shear of the mean zonal wind, the vertical propagation of these waves is disturbed, and ceases if the mean zonal wind comes close to the phase speed of the waves. A resulting net forcing on the zonal wind then takes place during the strong acceleration of the wind and the QBO or SAO Westerly phase is reinforced. In the case of an Easterly mean zonal wind, Kelvin waves are free to propagate and can attain significant amplitudes as their altitude increases. They break in the mesosphere, reduce the zonal wind speed and contribute to its reversal. Slow Kelvin waves that have not encountered a critical level are damped by thermal dissipation in the lower stratosphere.

The deep convection, particularly active at the tropical latitudes of interest, is assumed to be one of the main sources of the observed waves. Using a simplified model forced only by latent and convective heating Manzini and Hamilton (1993) found that latent heat release is by far the dominant excitation mechanism for the Kelvin waves. Hayashi (1994) proposed that equatorial waves result from wave-convection interactions and are intermittently triggered by random pulses of convective heating. Bergman and Salby (1994) used synoptic global cloud imagery, constructed from six satellites, to force the linearized primitive equations. Planetary-scale waves with periods longer than two days dominate the spectrum of geopotentiel. Hight-frequency gravity waves are also visible. They have a smaller variance but carry a larger fraction of the upward flux.

Tropical Kelvin waves are believed to contribute to the forcing of tropical westerly winds of both QBO (Holton and Lindzen 1972) and SAO (Hirota 1978), but smaller-scale gravity waves are also believed to play an important role (Dunkerton 1997), as Kelvin waves carry too little eastward momentum upwards to drive the QBO-westerlies.

This paper examines the structure of tropical winds and the strengths of the Kelvin waves in four free-running MACMs, along with the United Kingdom Meteorological Office analyses. In the first section we summarize the main characteristics of the SAO, QBO and Kelvin waves derived from observational fields. We then describe in the next section the data used for the comparative analysis which is detailed in the third one.

2 Characteristics of middle atmosphere variability

The SAO takes place in the upper stratosphere / lower mesosphere, between 1 and 0.1 hPa. Its features has been reviewed by Hirota (1980). The zonal winds blow alternately from East and West with a 6-month period. Near the stratopause the westerly wind maxima occur at the equinoxes and the easterly wind maxima at the solstices. The westerlies propagate downward with a speed of 6-7 km/month while the transition from westerlies to easterlies occurs simultaneously throughout a deep layer. Planetary wave activity, stronger during Northern than during Southern Hemisphere winter, causes a stronger easterly phase during the first SAO cycle (Delisi and Dunkerton 1988).

The QBO is also seen in stratospheric winds but occurs between 2 and 100 hPa, with a maximum amplitude near 10 hPa (Hamilton, 1981). This oscillation is characterized by an irregular period varying from 22 to 36 months. In the equatorial region where the QBO is dominant, easterly winds are typically 30 m/s and westerlies near 20 m/s. Alternating easterly and westerly wind regimes propagate downward, with the descent of easterly shear zones tending to propagate more slowly.

In the LIMS (Limb Infrared Monitor of the Stratosphere) data Hitchman and Leovy (1988) showed that the Kelvin waves seem to be excited by isolated events in the troposphere and propagate themselves into the middle atmosphere as wave packets. Their amplitude increases with height and when the zonal wind presents a strong East-West shear it can reach 4 - 5 K at 2 hPa during East-West SAO transitions and 3 - 4 K at 10 hPa during the East-West QBO transitions. In their analysis of a 15-year long radiosonde record collected in Singapore (1°N, 104°E), Shiotani and Horinouchi (1993) also noted a strong correlation between the Kelvin wave activity and the zonal wind acceleration as the QBO Westerly phase descends. More recently, the data obtained by instruments onboard UARS (Upper Atmosphere Research Satellite) also reveal the presence of Kelvin waves. Their maximum amplitude is 2 K in the low stratosphere and reaches 3 K between 5 and 1 hPa (Canziani et al. 1994, Shiotani et al. 1997). These various observations also reveal that, depending on the altitude, Kelvin waves have a zonal wavelength ranging from 30000 km to 40000 km (wave numbers 1 and 2), a vertical wavelength from 6 to 33 km, a period from 4 to 20 days and a phase velocity from 23 to 115 m/s. They are observed where winds are Easterlies or weak Westerlies. Their amplitude is amplified by both increasing altitude and strong East-West wind shear associated with a descent of the QBO or SAO Westerly phase. In this particular case, they will be more easily detected. Their amplitude is weaker in the low stratosphere. It is also weaker in the whole data set issued from the UARS observations than in the LIMS and radiosonde observations. Their activity varies over the course of the year. They seem to be episodically excited and appear in the form of isolated packets.

3 Data and method

Monthly-mean data collected by the team of the Free University in Berlin for the needs of EuroGRIPS have been used over a period of four years to compare SAOs and QBOs.

One year of higher frequency data necessary for the study of tropical waves were collected directly by the National Centre for Meteorological Research (CNRM). For each model as well as for the U.K. Meteorological Office (UKMO) analysed data, we have considered temporal three-dimensional series averaged over an equatorial band of temperature, zonal wind and meridional wind sampled every 4 hours, every 6 hours or every day. These data are described in Table 2.

The United Kingdom Meteorological Office assimilated data (Swinbank and O'Neil 1994) are sets of daily global meteorological analyses provided by the UKMO as their contribution to the UARS project. The data assimilation system is a development of the scheme used at the UKMO for operational weather forecasting, which has been extended to cover the stratosphere and has the potential to analyze a heterogeneous set of observational data (for example, NOAA satellite temperature profiles, radiosonde data, aircraft winds and temperatures). The numerical model used by the assimilation system is a stratosphere-troposphere configuration of the UKMO unified model (UM). The data fields are on the grid used by the numerical model with a north-south resolution of 2.5 °and an east-west resolution of 3.75 °. They are interpolated on standard UARS pressure levels from 1000 hPa to 0.3 hPa, with a vertical resolution in the stratosphere of approximately 1.6 km. For our study we have been provided with daily data from 1000 hPa to 1 hPa for the year 1994.

The models used for the intercomparison are the four troposphere-stratosphere MACMs of the EuroGRIPS project in which no constraints were imposed on boundary conditions.

An effort has been made to increase the vertical resolution of the models in the hope that they might then be able to resolve the shear zones and wave-mean flow interaction processes associated with the QBO. Under-scale phenomena as gravity waves which play an important role in the tropical forcing are parametrized in some models. The main characteristics of these models are presented below. We mention the gravity wave parametrization when it takes effect in the tropical region. More details could be found in the literature.

The UM of the U.K. Meteorological Office (UKMO) (Swinbank et al 1998) is a grid point model with a north-south resolution of 2.5 °and an east-west resolution of 3.75 °. Its vertical resolution is 1.3 km in the lower stratosphere with 29 levels between 300 and 10 hPa. A mesospheric Rayleigh friction is included;

The Troposphere-Stratosphere-Mesosphere (TSM) model of the Free University in Berlin (FUB) (Langematz and Pawson 1997) is a spectral model with a troncation T21 (5.6 °x 5.6 °). Its vertical resolution is 2-3 km in the lower stratosphere with 9 levels between 300 and 10 hPa. A mesospheric Rayleigh friction is included;

The ARPEGE-Climat model of the CNRM, Météo-France (Déqué et al 1994) is a spectral model with a troncation T21 (5.6 °x 5.6 °). Its vertical resolution is 1.5 km in the lower stratosphere with 14 levels between 300 and 10 hPa. A parametrization of gravity waves forced by convection (Bossuet et al. 1998) and mesospheric Rayleigh friction are included;

The Extended UGAMP GCM (EUGCM) of the Centre for Global Atmospheric Modelling (CGAM) (Norton and Thuburn 1996) is a spectral model with a troncation T42 (2.8 °x 2.8 °). Its vertical resolution is 1.3 km in the lower stratosphere with 12 levels between 300 and 10 hPa. A parametrization of gravity waves with non-zero phase speed is included.

As the zonal wind plays an important role in the initiation and propagation of Kelvin waves, vertical profiles of the zonal-mean zonal wind averaged over one or three months allowed us to interprete the different behaviours of these waves in the various models. Moreover, it helped in the choice of one or several cases worth closer study.

Both the linear theory of equatorial waves and observations agree in indicating that the temporal evolution of the temperature zonal wave number 1 (at a given longitude and averaged over a latitudinal band centered around the equator) provides some information about the Kelvin wave activity and vertical propagation. It must be stressed that these oscillations, characteristic of Kelvin waves, are of planetary scale in the zonal direction and have periods that are small compared to the analysed time period. In this case, the signal observed at any longitude may be considered as representative.

As we have just seen, the Kelvin wave propagation is directly determined by the zonal wind, which is itself very variable with the season as well as with the model.

Given these conditions, the period of study must be long enough. To investigate the period of time which provides statistically significant comparisons, a 10-year simulation of the ARPEGE-climat model has been scrutinized. To isolate spectral peaks associated with travelling equatorial waves, the spectral analysis was performed on overlapping 100 day time series centered on the 15th day of each month. Figure 1 shows the inter-annual variability of the eastward spectral density of temperature for a 12-day period. Power peaks occur more often during May-June when the zonal wind is westerly between 5 hPa and 30 hPa. Some years they occur in January and October. The differences in spectral peak intensity can be explained by the frequency of the occurence of the Kelvin wavetrains during the year. A comparison of time-height sections of temperature zonal wave 1 over the equator between the different year shows that the wave amplitude is similar. The analysis of a 10-year simulation of the ARPEGE-climat model allows us to conclude that one year seems to be an acceptable compromise to study the Kelvin waves.

The space-time analysis based on the Hayashi (1982) method is applied on selected case studies. 90-day temporal series of the temperature field have been analysed at several altitudes. This method allowed us to separate the spectral powers of Eastward and Westward waves. The spectral power distribution, as a function of the zonal wave number and the frequency, is compared to the theoretical dispersion curves and leads to the identification of the equatorial wave types that are present.

4 Results

4.1 Zonal wind and stratopause SAO

On Figure 2, the time series of the zonal-mean zonal wind near the equator in the four models are compared to the UKMO assimilated data.

The SAO and the QBO are evident in the assimilations but the models show large discrepancies. Nevertheless, each of them generates a semi-annual oscillation near the stratopause.

The Berlin model (TSM) reproduces rather realistic Easterly and Westerly phases but with a weak inter-annual variability.

In the Météo-France (ARPEGE-Climat) and Met Office (UM) models, an oscillation exists but it has an easterly bias. While in ARPEGE-Climat, the Westerlies maxima have an amplitude of 5 to 10 m/s (instead of 20 to 30 m/s) and are located between 1 and 10 hPa (compared to 0.5 hPa in the observation), in the UM they remain confined to the upper stratosphere (above 1 hPa) and have a very weak amplitude. In all three models (TSM, ARPEGE-Climat and UM), the Easterly phase is consistent with the climatology (Müller et al. 1997). although the summer phase is stronger than the winter phase in the latter two models.

Although the SAO simulated by the CGAM model (EUGCM) exhibits some unrealistic features in the stratosphere, it shows clear transitions from westerly to easterly winds near the stratopause; these are forced by imposed, parametrized gravity waves with non-zero phase speeds (Jackson 1995).

None of the models generates an Easterly or Westerly regime akin to a QBO. In the UM and TSM models, between 10 and 40 hPa, winds are always Easterly. In the ARPEGE-Climat model, weak Westerlies persist at these levels but there is no downward propagation. In the EUGCM model, a Westerly wind descent is initiated. but it has an annual period, weak amplitude and only descends to 30 hPa.

4.2 Kelvin waves in the UKMO assimilated data

The assimilated data are temporal series sampled every day (12 h UT) at the equator, on 19 levels distributed between 1000 and 1 hPa. The meridional resolution is 3.75 °. The year 1994 has been selected for the vertical and temporal structure of the zonal wind (Figures 2).

Over the selected time period, an Easterly phase of the QBO is diagnosed, with an East-West transition of the SAO above 3 hPa, prolonged by a descent of the QBO Westerly phase, well marked from September to the end of the year.

Figure 3 displays the temporal evolution of zonal wave number 1 at the grid-point 0 °N, 0 °E. Zonal mean zonal wind profiles averaged over one or three months drawn on the left panel of Figure 3 show that, in the analyses, wavetrains are present in May-June and September-October when East-West zonal wind shears are largest.

The April-May-June period corresponds to the SAO Westerly phase transition. The October-November-December period corresponds to a descent of the QBO Westerly phase (Figure 2).

For the first time period. the temperature spectral power has been computed at two different levels and plotted on Figure 4. The 10 hPa level corresponds to a zonal Easterly and the 1 hPa level to a full SAO Westerly phase with winds reaching 15 m/s in May. The straight lines on these figures correspond to theoretical dispersion curves for Kelvin waves propagating in a stationary atmodphere. Kelvin waves with phase velocities of 33 to 18 m/s, found at 10 hPa together with Easterlies, are damped when they enter Westerlies with speeds close to their own phase velocity. Figure 4 indicates that a rich spectrum of waves, eastward as well as westward are present in the assimilation, especialy at 1 hPa.

For the second period of time, Figure 5.a, b, c display the spectral power for the three levels 10 hPa, 32 hPa and 46 hPa respectively. The Kelvin wave theoretical dispersion curves have been superimposed on the spectral power. At 46 hPa. the zonal wind blows from the East over the whole period. Slow waves (11.5 to 16 m/s) as well as faster waves (23 to 46 m/s) are present at the same time. The 32 hPa level corresponds to a region where an important acceleration of the zonal wind takes place. The zonal wind varies from 0 to 10 m/s in the course of time and reaches 15 m/s locally. Figure 5.b shows that the spectral power is reinforced for waves with phase velocities ranging from 23 to 46 m/s.

Higher above, at 10 hPa, the slower waves has been attenuated and only fast waves are present.

Figure 6 displays time-longitude cross-sections of the temperature West and East components (separated by the Hayashi method) at different altitudes. In agreement with the spectral power diagrams of Figures 4 and 5, it is noticeable that the Westward component of zonal waves with small wave numbers and small frequencies is of the same order of magnitude as their Eastward component. This is even true over the entire spectral domain at higher altitudes. Figure 6. also provides some information about the temporal distribution of the waves at 32 hPa. In late October and early November. 10-day waves have a large amplitude where there is a strong wind shear. In mid-December. the zonal wind reaches 15 m/s and 7-day waves become predominant.

All these figures reveal that in the lower stratosphere, Eastward waves have periods of 15 to 20 days and maximum amplitudes of 2 K. At 10 hPa their periods are around 10 days and their amplitudes reach 2.5 - 3 K. The results are in reasonable agreement with those from the UARS MLS data (Canziani et al., 1994) and the UARS CLAES data (Shiotani et al., 1997).

4.3 Modelled Kelvin waves

Upward propagating wave 1 structures, identified as Kelvin waves are clearly visible in the temperature field of all four models (Figure 7). The interannual variability differs from model to model. It is much stronger than in the UKMO analyses or the UARS data. The synchronization between the downward propagation of the westerly winds maxima and the increase of the Kelvin wave amplitude is visible in all the modelsin in the upper stratosphere, especially in the EUGCM model during April-June.

Consistent with the observations, these waves propagate vertically in packets and their vertical wavelength (and hence their phase velocity) increases with altitude. In the UM, this variation is relatively weak and over the February-March period, the vertical wavelength remains practically constant over the whole stratosphere, with values smaller than for the other models.

The amplitude of the waves, in the UM model, is closest to the observed value from UARS (Shiotani et al., 1994). It is of 1 - 2 K in the low stratosphere, where winds blow from the East, and reaches 4 K in the high stratosphere during the periods January-March and August-October. These two periods correspond to acceleration of the SAO Westerly phases.

In the other three models, the Kelvin wave amplitudes reache 6 - 8 K in the high stratosphere where they exceed the observed amplitude and 3 - 4 K in the low stratosphere, where it is close to the wave amplitude observed by LIMS.

A case study has been performed for each of the models. The selected periods correspond to a strong wave activity associated either with a marked acceleration of the zonal wind or with a SAO Westerly phase. These periods are January-March for the UM and EUGCM models, February-April for TSM, and April-June for ARPEGE-Climat. Figure 8 show the temperature spectral power for two different levels in each model. Eastward waves are predominent in the temperature field so westward power spectral have not been drawn in these cases.

Kelvin waves with very slow phase velocities (16 m/s) are present in the UM and TSM models. They are filtered as they reach high altitudes and westerly zonal winds (5 m/s and 5 - 15 m/s respectively) (Figures 7 and 8a, c).

In agreement with both theory and observations, in three of the models (UM, TSM, EUGCM, Figure 7 and Figure 8.a, c, d respectively), the wave amplitude increases at around 1 hPa in the presence of a strong acceleration of the zonal wind, before being attenuated in the levels immediately above 1 hPa. The zonal wave number 1 gets strongly damped, particularly in the EUGCM model.

In the ARPEGE-Climat model, the maximum in the Westerlies appears at 10 hPa instead of 1 hPa and the wind gradients remain weak between 10 and 40 hPa (Figure 7 and 8.b). At 10 hPa, the zonal wind amplitude is 5 to 10 m/s and zonal wave number 1 component of the temperature field organises itself into cells with periods of 7 to 20 days and amplitudes of 6 to 7 K. The associated Kelvin waves have a phase velocity of 23 to 28 m/s and are unable to propagate above 10 hPa.

5 Discussion and conclusion

Comparison between zonal winds calculated by the four climate models reveals substantial differences. Nevertheless, a more or less realistic SAO is present in all models. In the UM, TSM and ARPEGE-climat models the SAO shows up as a half-yearly variation in the strength of the easterly winds. The vertical feature of the easterly phase of the three models is consistent with the climatology from Müller et al. 1997 but the inter-annual variability is too weak compared to the UKMO assimilations. Note that in contrast with the observations the easterly summer phase is stronger than the winter phase in the UM and ARPEGE-climat models.

Müller et al. 1997 found that the westerly phase in the TSM is due to easward propagating waves with a phase speed between 3.3 to 30 days. She found that thermal damping of the waves is under-estimated in the model which allows the slow waves to propagate too high in the atmosphere and therefore do not contribut to the forcing of the westerlies under 1 hpa.

Unlike the TSM, the westerlies of ARPEGE-climat are located between 1 and 10 hPa. Now the ARPEGE-climat model uses a simplified scheme to predict the ozone distributions in the middle atmosphere (Cariolle et all. 1990). The effects of ozone heating and photochemistry on forced equatorial Kelvin waves in shear flow has been examined by Echols and Terrence (1996). They showed that ozone heating produces an acceleration for a westerly sheared wind under 1 hPa and a decceleration above 1 hPa. But Westerlies produced in ARPEGE-climat stratosphere are yet too weak and do not reach the mesosphere. Note that the parametrization of gravity waves forced by convection included in this model affects only a little the equatorial stratosphere.

Although the SAO simulated in the EUGCM exhibits the easterly phase with some unrealistic features, it shows clear transitions from westerly to easterly winds near the stratopause; these are forced by imposed, parametrized gravity waves with non-zero phase speed.

None of the models reproduces any East or West system that resembles the observed QBO. In the UM and TSM, between 10 and 40 hPa, winds are always easterly. In ARPEGE-Climat, a weak Westerly system exists at these levels but at first sight without neither the correct downward propagation nor the good period. Cariolle et al. 1993 still showed that it can be seen as a QBO signal. The EUGCM initiates a realistic descent of the Westerlies of about 1 km/month between 10 and 30 hPa, but its amplitude is too weak and has an annual period.

In the assimilations a rich spectrum of waves (eastward and westward) are present and help to drive the SAO and the QBO. Eastward and westward waves have similar amplitudes.

Kelvin waves have periods of 7 to 20 days and their amplitude is close to the amplitude observed by UARS. Slow 30-day waves are also present in the lower stratosphere. These waves are consistent with the linear theory of equatorial waves.

All four models studied here are able to generate Kelvin waves that appear to be excited by isolated tropospheric events and to propagate into the middle atmosphere as wave packets underlining to a relationship with convective forcing. The Kelvin waves amplitude is larger in the TSM, ARPEGE-Climat and EUGCM models, but remains comparable to the LIMS satellite data in the lower stratosphere. In the upper stratosphere and in the mesosphere, Kelvin waves are overestimated by these three models. They are close to the UARS satellite measurements in the UM model, but these differencies between the UM and the others can be explained by the fact that it is a grid point model and hence more diffusif.

Models show more eastward propagating wave activity than the UKMO assimilated data. These eastward waves can propagate around the globe.

To confirm the connection between the underlying convection and the wave activity emerging at tropopause level, we compared the convective rain field with the Kelvin waves activity in the 10-year simulation of the ARPEGE-climat model. For each month the convective rain field as well as the eastward waves power spectra have been averaged over the ten years of the simulation. At 100 hPa an eastward 32-day wave domines the spectrum of temperature. Its variance is maximum during March at 100 hPa when a peack in convective rain occurs over the east of the Indian Ocean. A weaker maximum of the 12-day Kelvin wave variance occurs during April-May at 100 hPa when the convective rain is maximum over the Indonesia, Pacifique Ocean, America and Africa. It increases and moves in May-June with height showing a vertical propagation of the Kelvin wave. Another peak in the Kelvin wave variance occurs during October when strong convective rains are over the Indian Ocean, America and Africa. Here also deep convection over the eastern Indian Ocean acts as a trigger.

Westward waves are superimposed on Kelvin waves in the UKMO analyses, which makes their detection more difficult. This is not the case in the various models. Moreover, the zonal wind variability due to the presence of a QBO in the UKMO analyses perturbs the vertical propagation of Kelvin waves and favours the simultaneous presence of Eastward and Westward waves. An interaction between these waves of opposite directions may also perturb the horizontal propagation of Kelvin waves. The conjunction of these two phenomena prevents Kelvin wavetrains from organizing. Because of the absence of a QBO in the models, Kelvin waves are not absorbed in the lower stratosphere and propagate up to the mesosphere. Though they are overestimated in the upper stratosphere and mesosphere they are not sufficient to force westerly winds at these levels.

Horinouchi and Yoden (1998) found that realistic structures in cumulus convection were able to excite a complete range of waves, from small to planetary scales which were required for forcing the QBO. They mention also the importance of small enough vertical spacing (500m- 700m) to solve the small vertical wavelengths of waves approaching a critical level.

The results of the intercomparison are consistent with the view that a wide range of waves, especialy small-scale waves not resolved by the models, a realistic convection and an appropriate thermal damping are required for forcing the QBO and for the adequate generation of the SAO.

Acknowledgements:

The model intercomparison has been funded by the European Framewrok IV "Euro-GRIPS" Project (ENV4-ST95-0123). MA is grateful to Anne De Rudder for her help in translating the original paper. She thanks Serge Planton, and Martine Michou for their useful comments on the manuscript.

REFERENCES

Bergman, J. W., and M. L. Salby. 1994: Equatorial wave activity derived from fluctuations in observed convection. J. Atmos. Sci., 51, 3791-3806.

Bossuet, C., M. Déqué, and D. Cariolle, 1998: Impact of a simple parametrization of convective gravity-wave drag in a stratosphere-troposphere general circulation model and its sensitivity to vertical resolution. Ann. Geophysicae,16,238-249.

Canziani, P., and J.R. Holton, 1994: Equatorial Kelvin waves: A UARS MLS view, J. Atmos. Sci., 51. 3053.

Delisi, D. P. and T. J. Dunkerton, 1988: Seasonal variation of the semiannual oscillation. J. Atmos. Sci., 45, 2772-2787.

Déqué, M., C. Dreveton, A. Braun, D. Cariolle, 1993: The ARPEGE/IFS atmosphere model: a contribution to the French community climate modelling. Climate Dyn.,10:249-266.

Hamilton, K., 1981: The vertical structure of the quasi-biennial oscillation : Observations and theory, Atmos. Ocean, 19,236-250.

Hayashi, Y., and D. G. Golder 1994: Kelvin and mixed Rossby-Gravity waves appearing in the GFDL "SKYHI" general circulation model and the FGGE dataset: Implications for their generation mechanism and role in the QBO. J. Meteor. Soc. Japan, 72, 901-935.

Hayashi, Y., 1982: Space-time spectral analysis and its application to atmospheric waves. J. Meteor. Soc. Japan, 60, 156-171.

Hirota, I., 1978: Equatorial waves in the upper stratosphere and mesosphere in relation to the semiannual oscillation of the zonal wind. J. Atmos. Sci., 35, 714-722.

——, 1979: Kelvin waves in the equatorial middle atmosphere observed by the Nimbus 5 SCR. J. Atmos. Sci., 36, 217-222.

——, 1980: Ibservational evidence of the semiannual oscillation in the tropical middle atmosphere– A review.Pure Appl. Geophys., 118, 217-238.

Hitchman, M.H., and C.B. Leovy,1988: Estimation of the Kelvin wave contribution to the semiannual oscillation, J. Atmos. Sci., 45, 1462-1475.

Holton, J.R., 1975: The dynamic Meteorology of the stratosphere and mesosphere, Meteor. Monogr., No. 37, Am Meteor. Soc., Boston, Massachusetts.

——, and R.S. Lindzen, 1972: An updated theory for the quasi-biennal cycle of the tropical stratosphere. J. Atmos. Sci., 29, 1076-1080.

Horinouchi, T., and S. Yoden, 1997: Wave mean flow interaction associated with a QBO-like oscillation in a simplified GCM. J. Atmos. Sci., 55, 502-526.

Langematz, U., and S. Pawson, 1997: The Berlin troposphere-stratosphere-mesosphere GCM: Climatology and forcing mechanisms. Q.J.R. Meteorol.Soc., 123,1075-1096.

Lindzen, R.S., and J.R. Holton, 1968: A theory of the quasi-biennial oscillation. J. Atmos. Sci., 25, 1095-1107.

Mahlman, J. D., and L. J. Umscheid, 1984: Dynamics of the middle atmosphere: successes and problems of the GFDL "SKYHI" general circulation model. In "Dynamics of the Middle Atmosphere." (J. R. Holton and T. Matsuno, eds), pp. 501-525. Terrapub,Tokyo.

Manzini E., and K. Hamilton, 1993: Middle atmospheric travelling waves forced by latent and convective heating. J. Atmos. Sci., 50, 2180-2200.

Müller, K.M., U. Langematz, and S. Pawson, 1997: The stratopause semiannual oscillation in the berlin troposphere-stratosphere-mesosphere GCM, J. Atmos. Sci., 54, 2749-2759.

Norton and Thuburn, 1996: The mesosphere in the Extended UGAMP GCM. In 'Gravity wave processes and their parametrization in global climate models'. Ed. K. Hamilton, Springer-Verlag.

Pawson, S., K. Kodera, K. Hamilton, T.G. Shepherd, S.R. Beagley, B.A. Boville, J.D. Farrara, T.D.A. Fairlie, A. Kitoh, W. Lahoz, U. Langematz, E. Manzini, D.H. Rind, A.A. Scaife, K. Shibata, P. Simon, R. Swinbank, L. Takacs, R.J. Wilson, J.A. Al-Saadi, M. Amodei, M. Chiba, L. Coy, J. de Grandpré, R.S. Eckman, M. Fiorino, W.L. Grose, H. Koide, J.N. Koshyk, D. Li, J. Lerner, J.D. Mahlman, N.A. McFarlane, C.R. Mechoso, A. Molod, A. O'Neill, R.B. Pierce, W.J. Randel, R.B. Rood, F. Wu, 1999: The GCM-Reality Intercomparison Project for SPARC (GRIPS): Scientific Issues and Initial Results. Bull. Am. Meteorol. Soc., in press (March 2000).

Reed, R. J., 1966: Zonal wind behavior in the equatorial stratosphere and lower mesosphere. J. Geophys. Res., 71, 4223-4233.

Salby, M.L., and D.L. Hartmann, P. L. Bailey, and J. C. Gille, 1983: Evidence for equatorial Kelvin waves in Nimbus-7 LIMS. J. Atmos. Sci., 41, 220-235.

Shiotani, M., and T. Horinouchi, 1993: Kelvin waves activity and the quasi-biennial oscillation in the equatorial lower stratosphere, J. Meteor. Soc. Japan, 71, 175-181.

——, J.C. Gille, and A. E. Roche, 1997: Kelvin Waves in the equatorial lower stratosphere as revealed by cryogenic limb array etalon spectrometer temperature data. J. Geophys. Res., 102, 26,131-26.140.

Takahashi, M., 1996: Simulation of the stratospheric quasi-biennial oscillation using a general circulation model. Geophy. Res. Lett., 23, 661-664.

Swinbank, R., W. Lahoz, A. O'Neill, C. S. Douglas, A. Heaps and D. Podd, 1998: Middle atmosphere variability in the UK Meteorological Office Unified Model, Q.J.R. Meteorol. Soc., 124,1485-1525.

——, and A. O'Neill, 1994: A stratosphere-troposphere data assimilation system. Monthly Weather Review, 122, 686-702.

Wallace, J., and V. Kousky, 1968a: Observational evidence of Kelvin waves in the tropical stratosphere. J. Atmos. Sci., 25, 900-907.

——, 1973: General circulaton of the tropical lower stratosphere. Rev. Geophys. Space Phys., 2 191-222.

UKMO **UM**	**FU-Berlin** **TSM**	**Météo-France(CNRM)** **ARPEGE-climat V2**	**CGAM** **EUGCM**	**UKMO** **Analyses**
Grid points (2 °5x3 °75) 49 levels	Spectral T21 (5 °6x5 °6) 37 levels	Spectral T21 (5 °6x5 °6) 41 levels	Spectral T42 (2 °8x2 °8) 47 levels	Grid points (2 °5x3 °75)
Domain: 1000 $\longrightarrow$ 0.1hPa	Domain: 1000 $\longrightarrow$ 0.01hPa	Domain: 1000 $\longrightarrow$ 0.05hPa	Domain: 1000 $\longrightarrow$ 0.01hPa	Domain: 1000 $\longrightarrow$ 1 hPa
Every 6 h	Every 4 h	Every 6 h	Every 6 h	Every day 12h UTC
Latitudes: 3 °75N, 1 °25N, 1 °25S, 3 °75S	Latitudes: 2 °8N-2 °8S	Latitudes: 2 °8N-2 °8S	Latitudes: 1 °4N-1 °4S	Latitude: 0 °

Table 2

Figures captions:

Figure 1: Time serie over 10 years of the spectral power of temperature fluctuations of zonal-wave number 1 and 12-day period during the period January 1979 to October 1988. The contour interval is 0.002 K^2. First contour is 0.01 K^2.

Figure 2: Time series over four years of the zonal-mean zonal wind near the equator in the UKMO assimilated data and the TSM, ARPEGE-climat, EUGCM and UM models (top to bottom). Negative values (easterlies) are shaded and the contour interval is 10 m/s. The vertical axis extends from the surface to 0.2 hPa. The four selected years for the UKMO assimilated data are 1992 to 1996.

Figure 3: Time-height section of temperature zonal wave 1 over the equator at 0° longitude for the UK Met Office assimilated data for the year 1994. Positive values are shaded and the contour interval is 0.5 K. The solid lines of the left panel show the zonal wind averaged over the 3 months of the right panels; dotted lines correspond to the first month, dashed lines to the second month and dash-dotted lines to the third month.

Figure 4: Frequency-wavenumber power spectrum of the temperature field of the UK Met Office assimilated data. over the equator, for the time period April to June at 1 hPa (a) and 10 hPa (b). The contour interval is 0.05 K^2.

Figure 5: Frequency-wavenumber power spectrum of the temperature field of the UK Met Office assimilated data. over the equator, for the time period October to December at 10 hPa (a), 32 hPa (b) and 46 hPa (c). The contour interval is 0.05 K^2.

Figure 6: Time-longitude section of the eastward (left) and westward (right) temperature deviation from the zonal average of the UK Met Office assimilated data over the equator for the time period (a) Apr-Jun at 10 hPa and (b) Oct-Dec at 32 hPa. Positive values are shaded and the contour interval is 0.5 K.

Figure 7: Time-height section of temperature zonal wave 1 average over an equatorial band at 0°longitude for the time period Jan-Mar (a) and Apr-Jun (b) for the UM, ARPEGE-climat, TSM and EUGCM models. Positive values are shaded and the contour interval is 1 K. The solid lines of the left panel show the zonal wind profiles averaged over the 3 months Jan-Feb-Mar (a) and Apr-May-Jun (b); dotted lines correspond to January and April, dashed lines to February and May and dash-dotted lines to March and June.

Figure 8: Frequency-wavenumber power spectrum of the temperature field of the 4 models over and equatorial band;
a) UM model for the time period Jan-Mar at 1 hPa (left) and 0.3 hPa (right),
b) ARPEGE-climat model for the time period Apr-Jun at 10 hPa (left) and 1 hPa (right),
c) TSM for the time period Feb-Apr at 1 hPa (left) and 0.2 hPa (right),
d) EUGCM model for the time period Jan-Mar at 2 hPa (left) and 0.3 hPa (right).
The contour interval is 1 K^2.

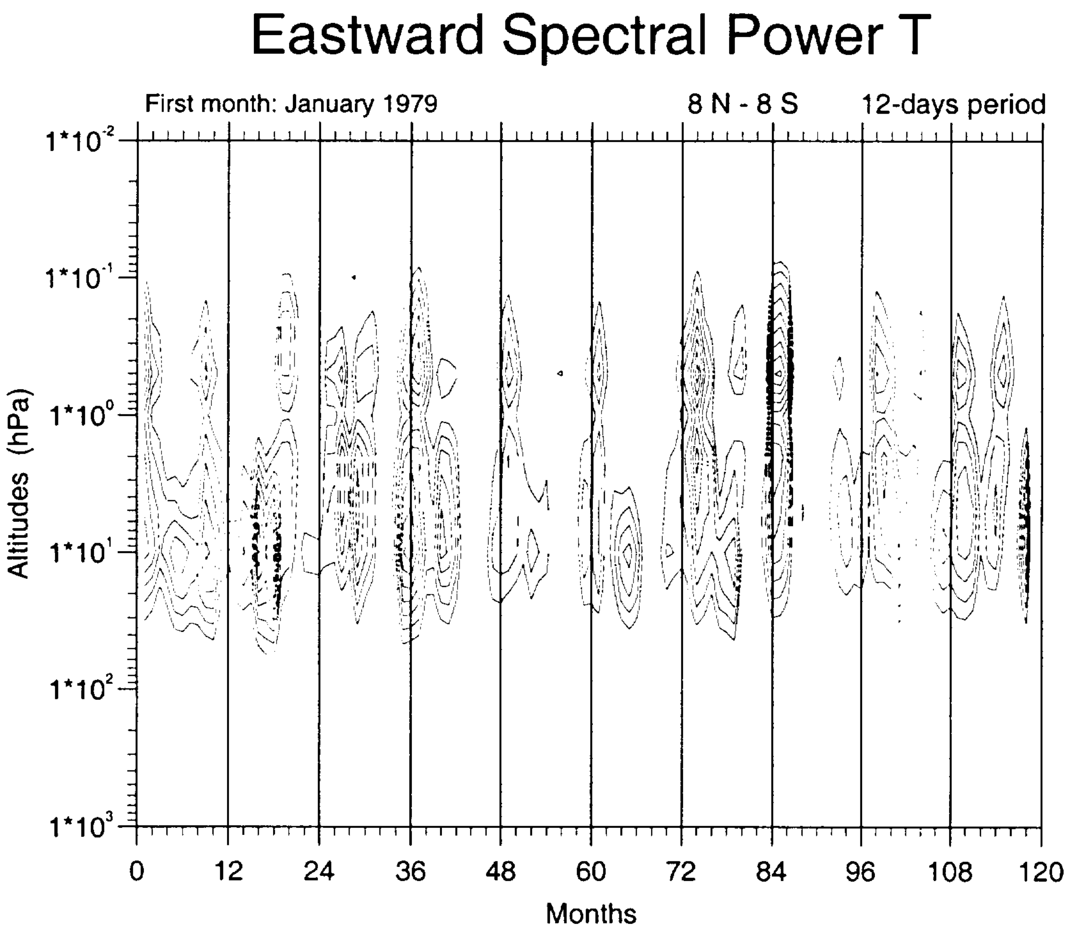
Eastward Spectral Power T
First month: January 1979
8 N - 8 S
12-days period
Altitudes (hPa)
1*10^-2
1*10^-1
1*10^0
1*10^1
1*10^2
1*10^3
0
12
24
36
48
60
72
84
96
108
120
Months

Fig. 1

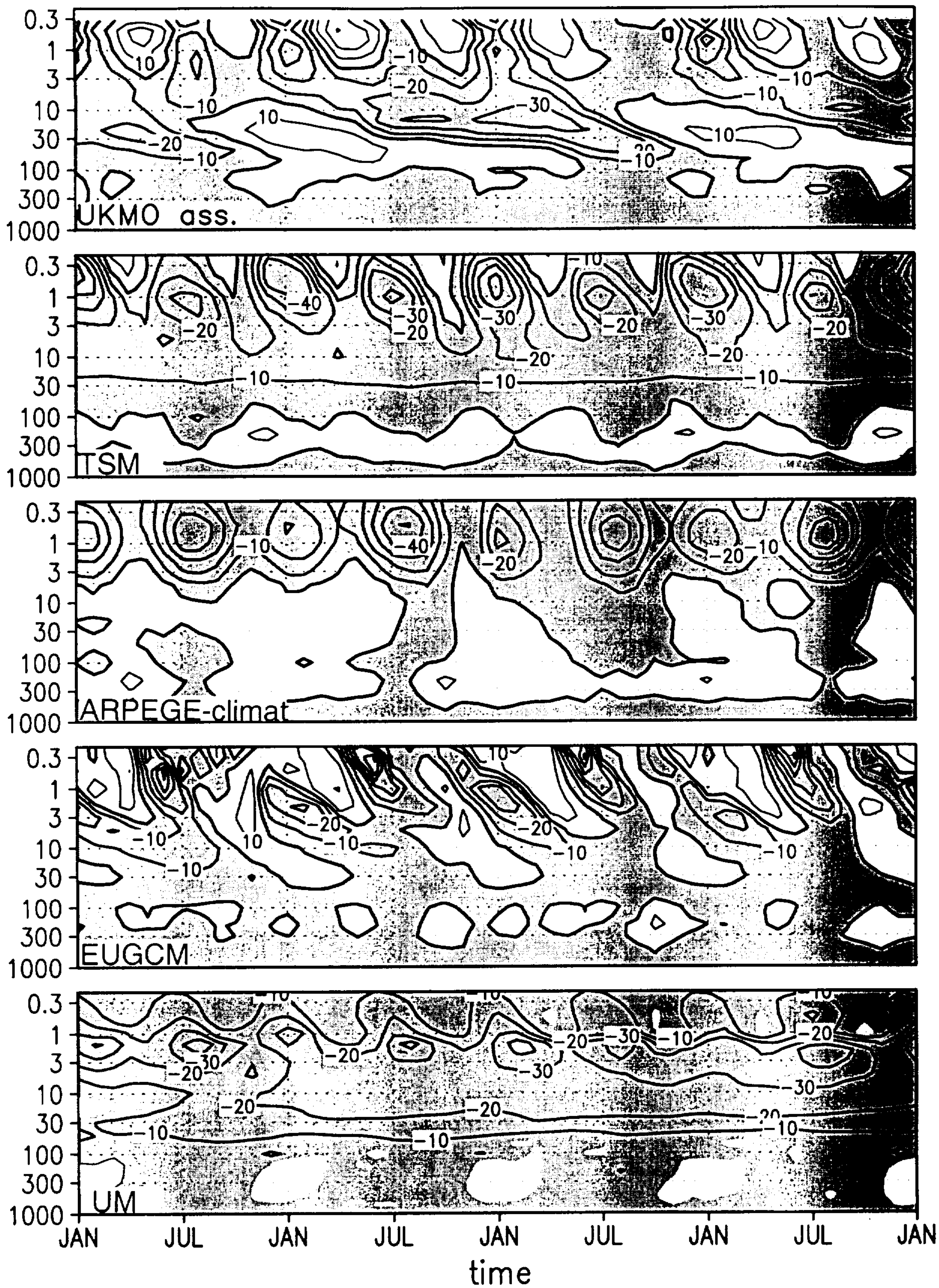
UKMO ass.
TSM
ARPEGE-climat
EUGCM
UM
0.3
1
3
10
30
100
300
1000
JAN
JUL
JAN
JUL
JAN
JUL
JAN
JUL
JAN
time

Fig.2

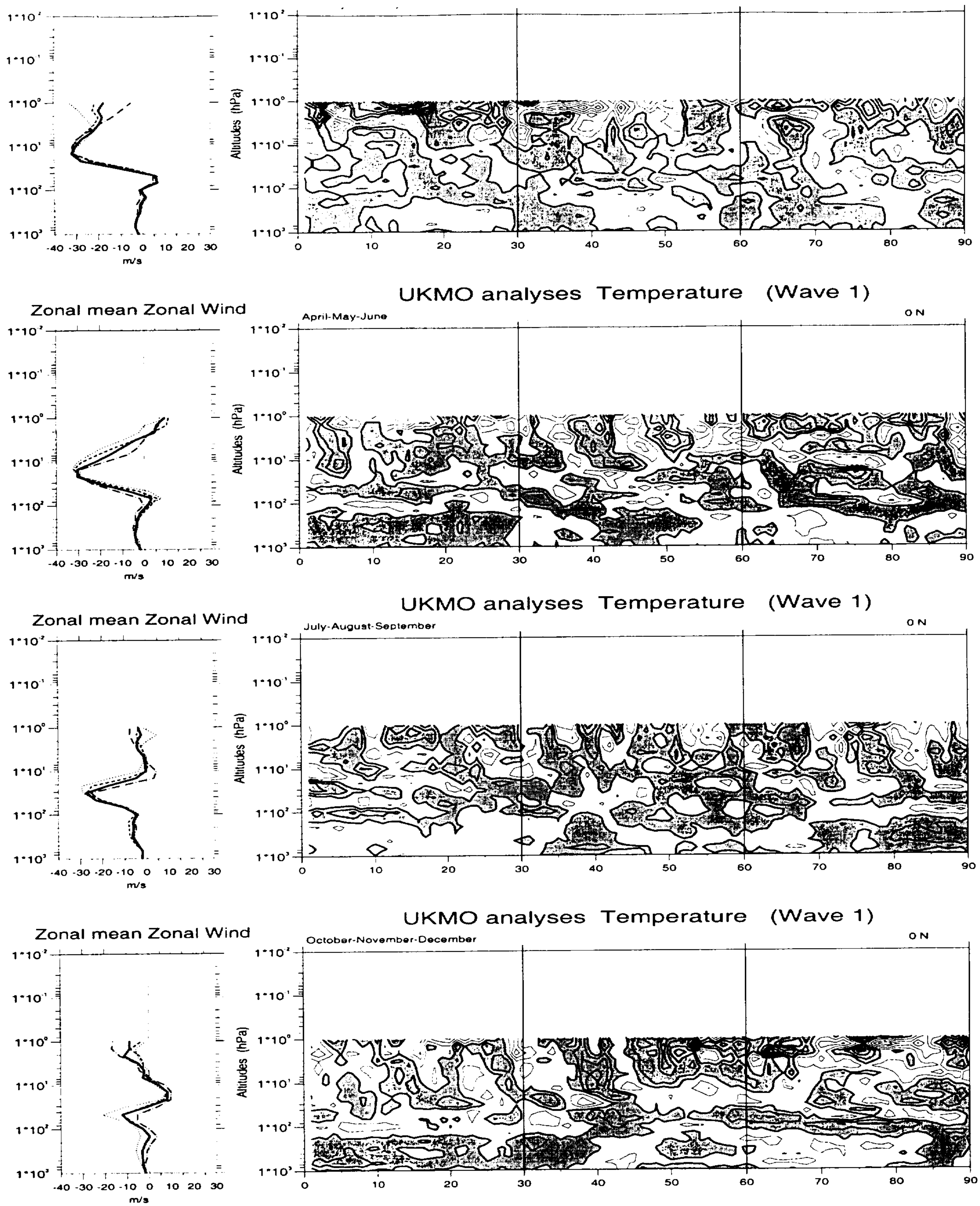
Zonal mean Zonal Wind
UKMO analyses Temperature (Wave 1)
April-May-June
0 N
July-August-September
October-November-December
Altitudes (hPa)
m/s
-40 -30 -20 -10 0 10 20 30
0 10 20 30 40 50 60 70 80 90

Fig. 3

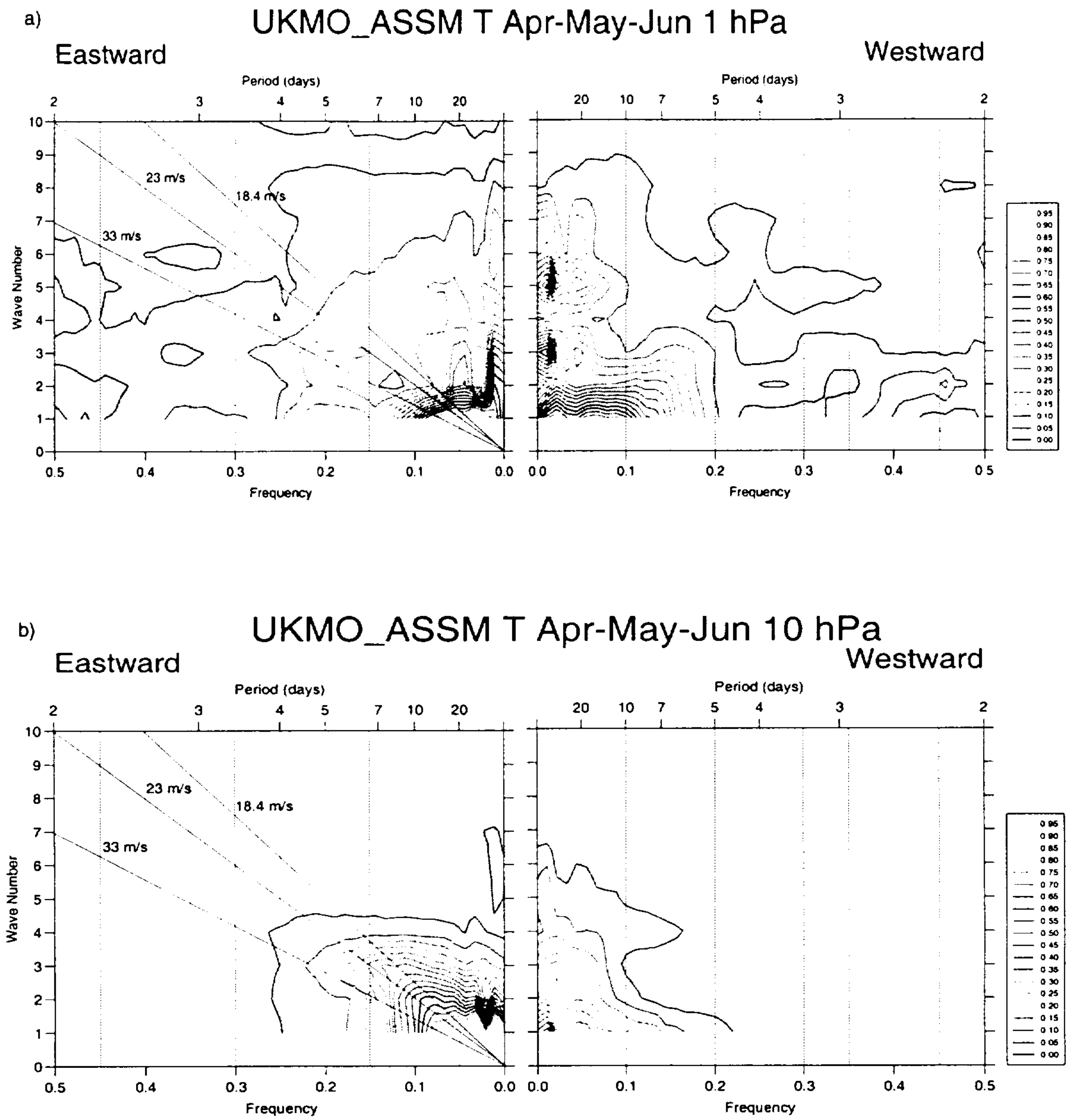
a)
UKMO_ASSM T Apr-May-Jun 1 hPa
Eastward
Westward
Period (days)
Wave Number
Frequency
23 m/s
18.4 m/s
33 m/s
b)
UKMO_ASSM T Apr-May-Jun 10 hPa
Eastward
Westward
Period (days)
Wave Number
Frequency
23 m/s
18.4 m/s
33 m/s

Fig. 4

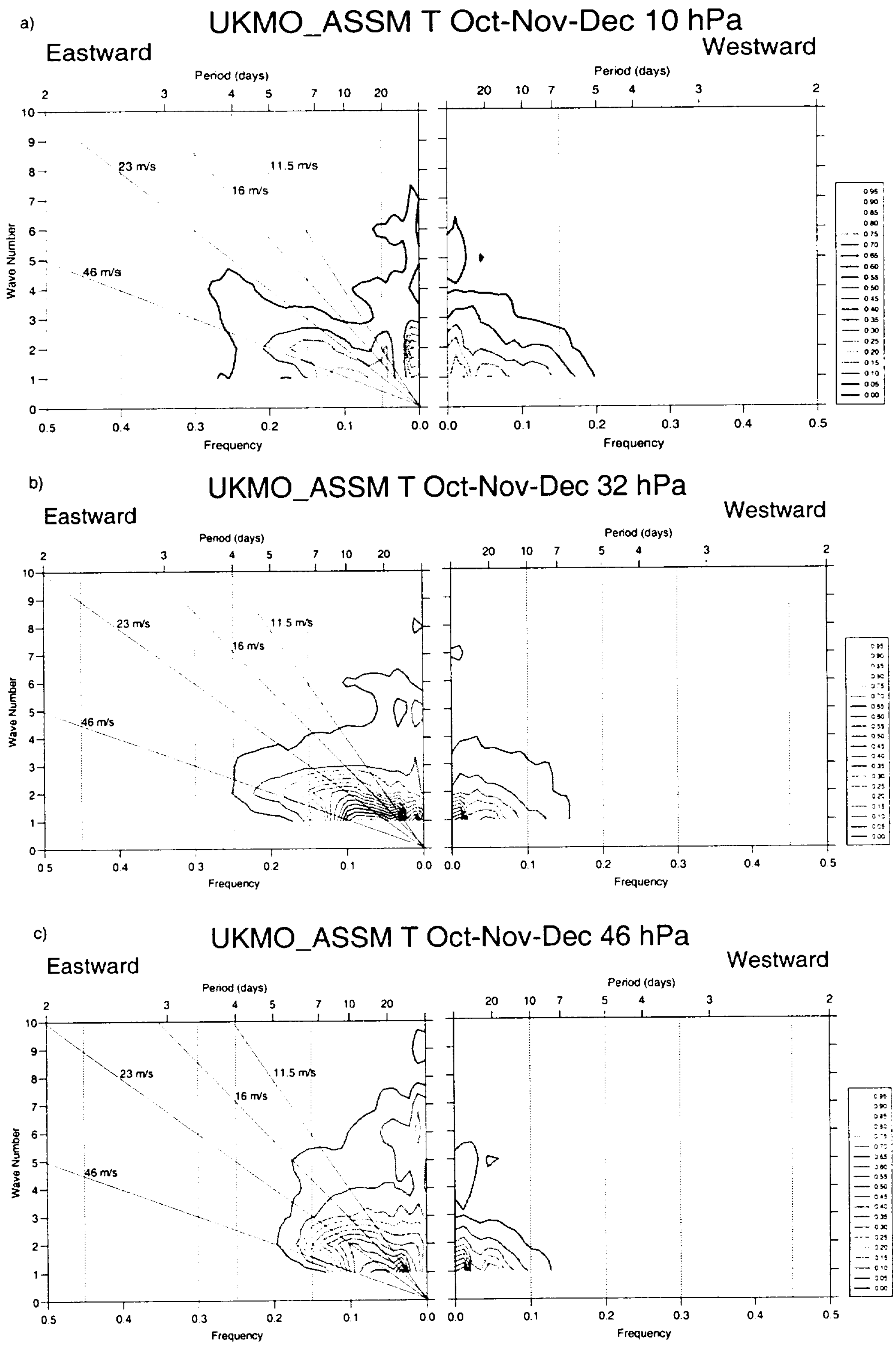

a)
UKMO_ASSM T Oct-Nov-Dec 10 hPa
Eastward
Westward
Period (days)
Wave Number
Frequency
23 m/s
11.5 m/s
16 m/s
46 m/s
b)
UKMO_ASSM T Oct-Nov-Dec 32 hPa
Eastward
Westward
Period (days)
Wave Number
Frequency
23 m/s
11.5 m/s
16 m/s
46 m/s
c)
UKMO_ASSM T Oct-Nov-Dec 46 hPa
Eastward
Westward
Period (days)
Wave Number
Frequency
23 m/s
11.5 m/s
16 m/s
46 m/s

Fig.5

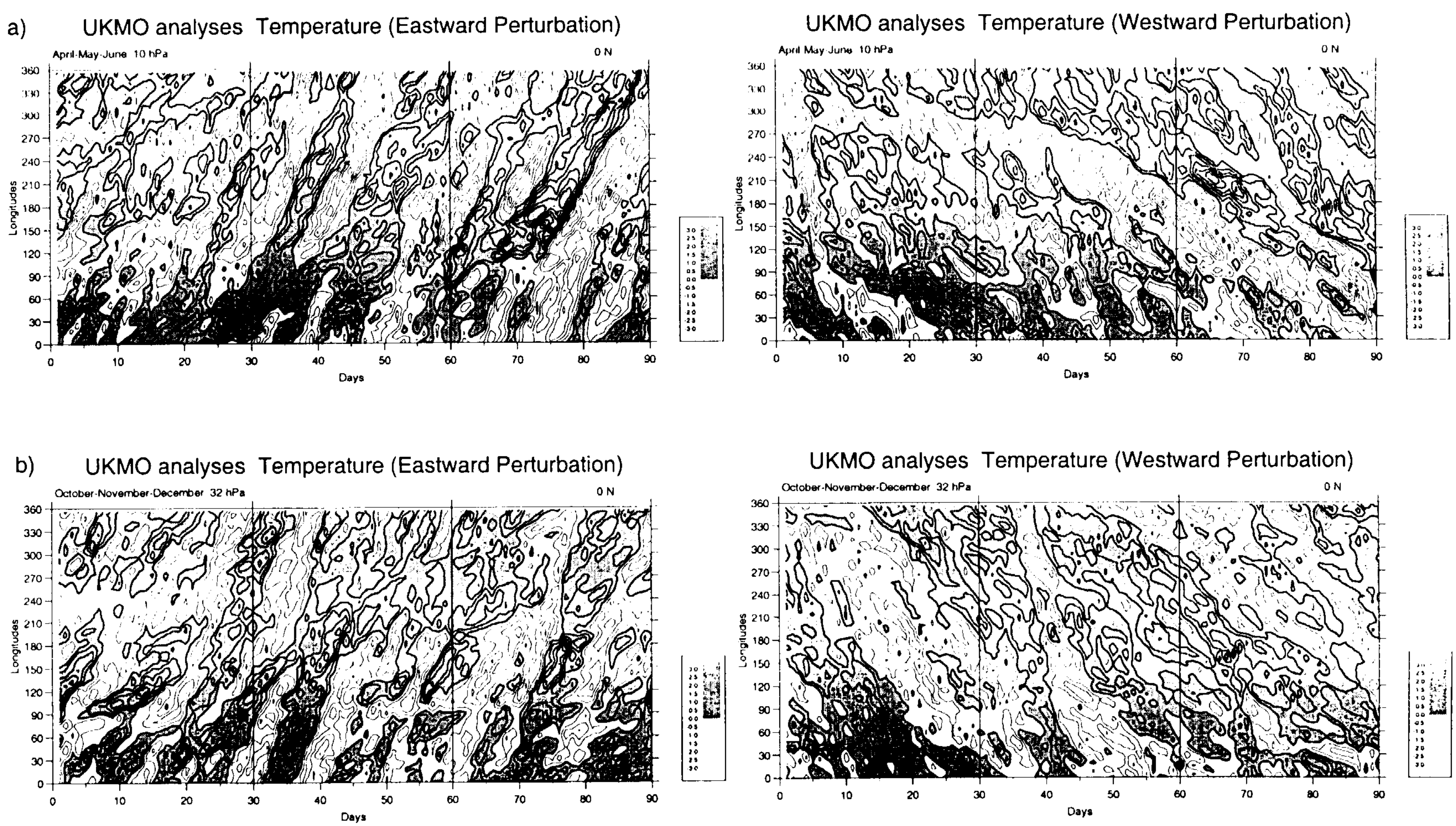
a)
UKMO analyses Temperature (Eastward Perturbation)
April-May-June 10 hPa
0 N
Longitudes
Days
UKMO analyses Temperature (Westward Perturbation)
April May June 10 hPa
0 N
Longitudes
Days
b)
UKMO analyses Temperature (Eastward Perturbation)
October-November-December 32 hPa
0 N
Longitudes
Days
UKMO analyses Temperature (Westward Perturbation)
October-November-December 32 hPa
0 N
Longitudes
Days

Fig. 6

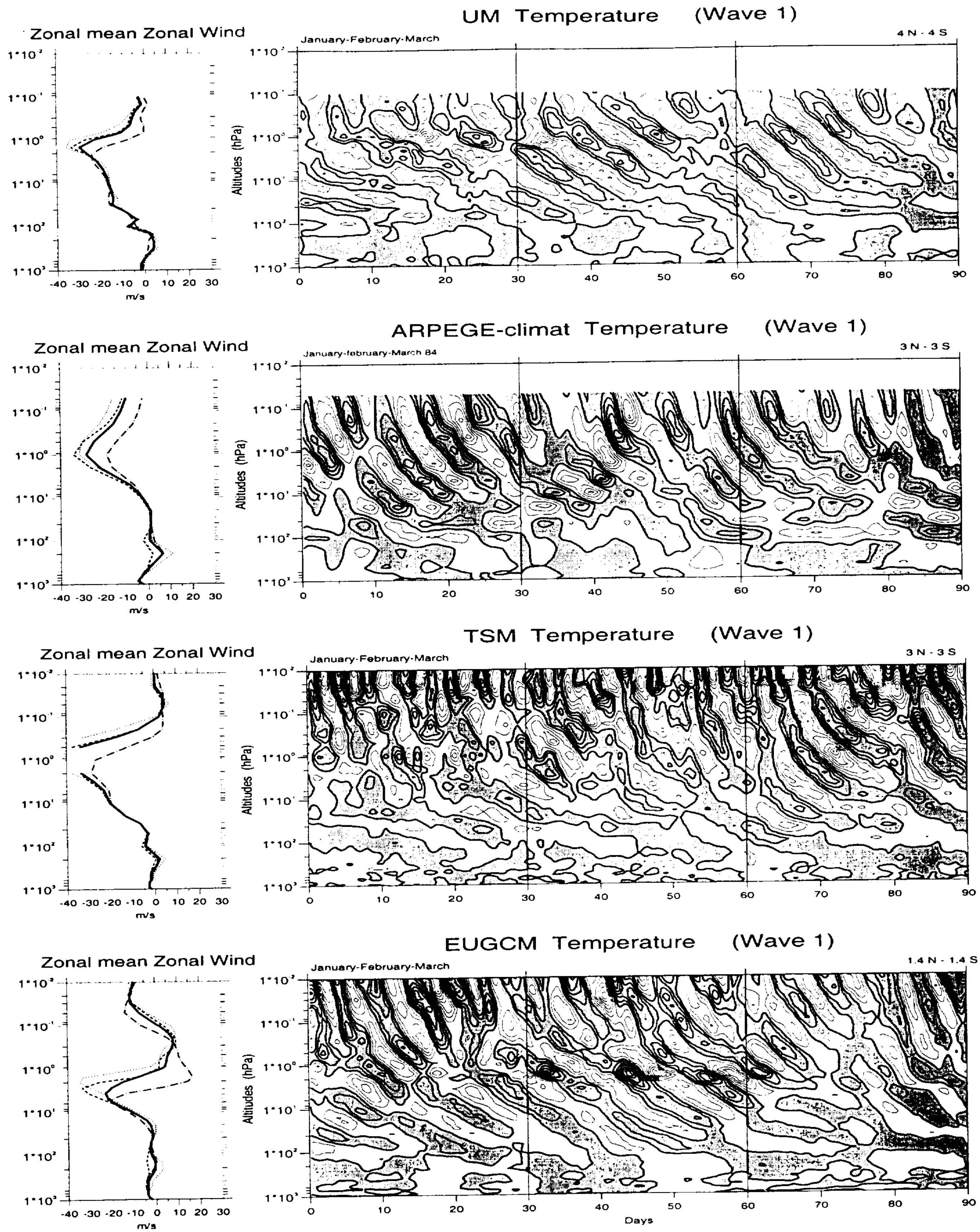
UM Temperature (Wave 1)
Zonal mean Zonal Wind
January-February-March
4 N - 4 S
Altitudes (hPa)
m/s
ARPEGE-climat Temperature (Wave 1)
Zonal mean Zonal Wind
January-february-March 84
3 N - 3 S
Altitudes (hPa)
m/s
TSM Temperature (Wave 1)
Zonal mean Zonal Wind
January-February-March
3 N - 3 S
Altitudes (hPa)
m/s
EUGCM Temperature (Wave 1)
Zonal mean Zonal Wind
January-February-March
1.4 N - 1.4 S
Altitudes (hPa)
m/s
Days

Fig.7

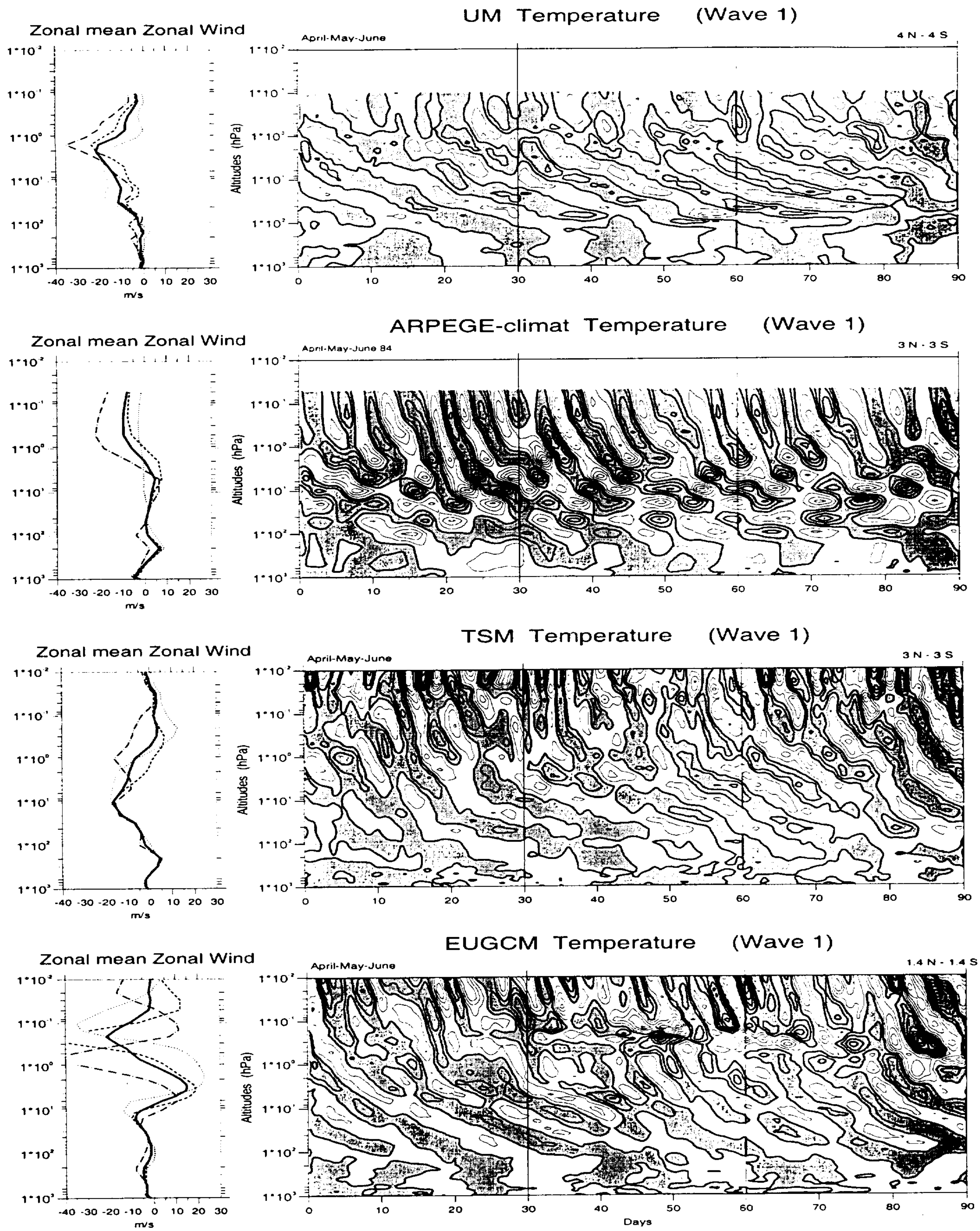

Fig.7 (continued)

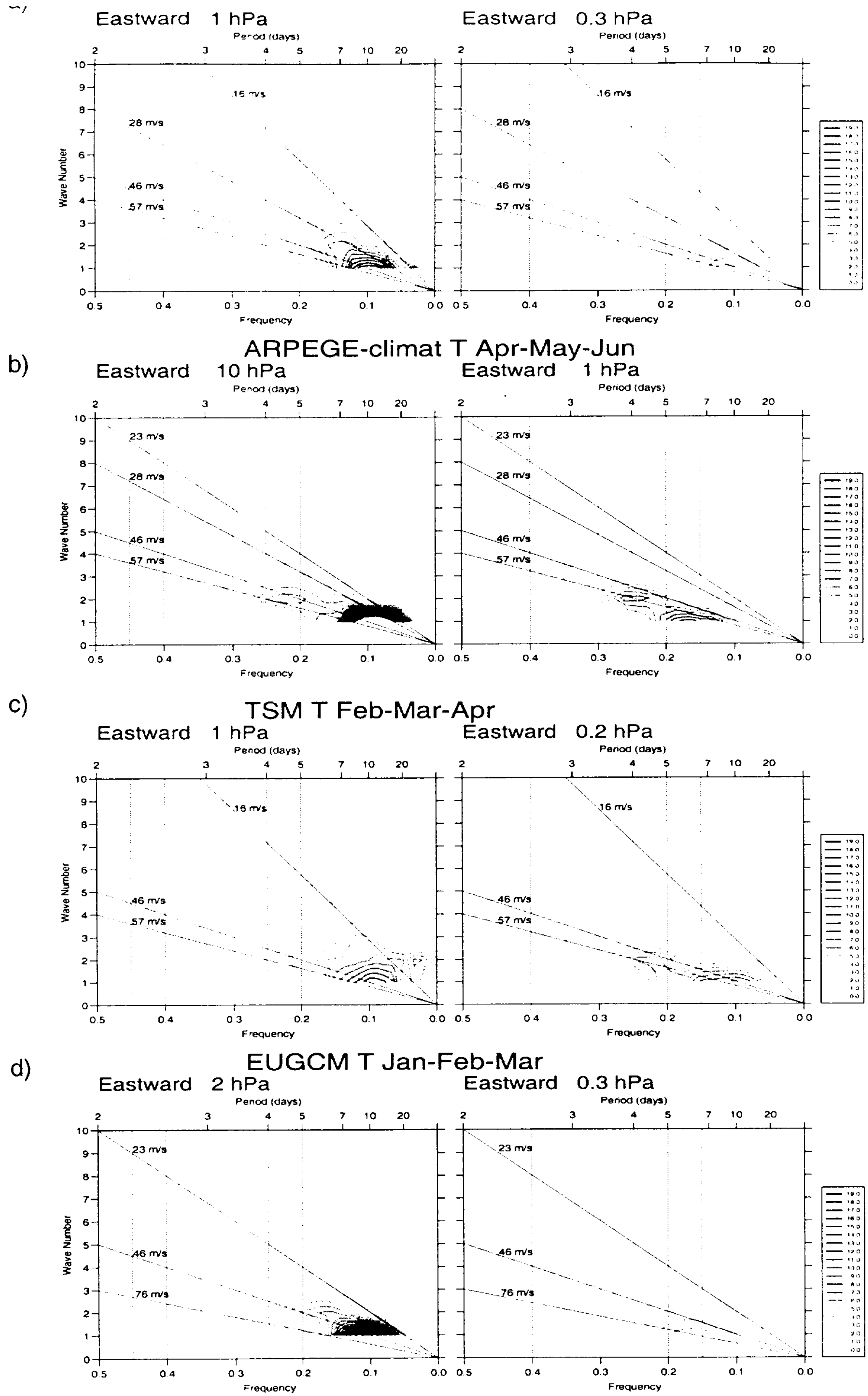

Eastward 1 hPa
Eastward 0.3 hPa
Period (days)
Wave Number
Frequency
16 m/s
28 m/s
46 m/s
57 m/s
b)
ARPEGE-climat T Apr-May-Jun
Eastward 10 hPa
Eastward 1 hPa
23 m/s
28 m/s
46 m/s
57 m/s
c)
TSM T Feb-Mar-Apr
Eastward 1 hPa
Eastward 0.2 hPa
16 m/s
46 m/s
57 m/s
d)
EUGCM T Jan-Feb-Mar
Eastward 2 hPa
Eastward 0.3 hPa
23 m/s
46 m/s
76 m/s

Fig. 8